

Simulation of positive streamers in CO₂ and in air: the role of photoionization or other electron sources

Behnaz Bagheri^{1,2}, Jannis Teunissen¹, and Ute Ebert^{1,2}

¹Centrum Wiskunde & Informatica (CWI), Amsterdam, The Netherlands

²Technical University of Eindhoven, Eindhoven, The Netherlands

E-mail: b.bagheri@tue.nl

5 October 2020

Abstract. Positive streamer discharges have been studied and modelled extensively in air. Here we study positive streamers in CO₂ with and without oxygen admixtures; they are relevant for current high voltage technology as well as for discharges in the atmosphere of Venus. We discuss that no efficient photoionization mechanism is known for gases with a large CO₂ fraction, as photons in the relevant energy range are rapidly absorbed. Hence positive streamers can propagate only due to some other source of free electrons ahead of the ionization front. Therefore we study positive streamer propagation in CO₂ with different levels of background ionization to provide these free electrons. The effect of replacing photoionization by background ionization is studied with simulations in air. Simulating streamers in background fields of 16 to 20 kV/cm at standard temperature and pressure within a gap of 6.4 cm, we find that streamer propagation is rather insensitive to the level of photoionization or background ionization. We also discuss that the results depend not only on the value of breakdown field and applied electric field, and on preionization or photoionization, but also on the electron mobility $\mu(E)$ and the effective ionization coefficient $\alpha_{\text{eff}}(E)$, that are gas-dependent functions of the electron energy or the electric field.

1. Introduction

1.1. Positive streamers in air and other $N_2:O_2$ mixtures

Streamers are rapidly growing ionized filaments which govern the initial phase of electric breakdown; they later can develop into a spark or a lightning leader [1–4]. Their growth is governed by the curved space charge layer around their tips which enhances the electric field in the non-ionized areas in front of them and allows them to penetrate into areas where the background electric field is below the breakdown threshold. They are weakly ionized channels, hence they do not increase the gas temperature significantly. We focus here on positive streamers that start and propagate more easily in air than negative streamers. Positive streamers propagate in the direction of the electric field with velocities comparable to the local electron drift velocity, but in the opposite direction, therefore they require a source of free electrons in front of their head to sustain their growth. In $N_2:O_2$ mixtures like air, these electrons are provided by photoionization [5,6]. Background ionization, e.g., from previous discharges, can further influence their growth. In the present paper, the role of photoionization or other electron sources for positive streamer propagation will be investigated, in particular, in CO_2 with or without admixtures of other gases.

Streamers are used in numerous applications in plasma technology [7,8], for instance for the production of chemical radicals [9], in ignition and combustion [10] and in plasma catalysis [11].

1.2. Positive streamers in CO_2 with or without admixtures

In the present work, we concentrate on properties of positive streamers in CO_2 . The study is motivated by current needs in high-voltage technology, where pressurized gas is used for insulation and current interruption purposes [12–14]. The commonly used working gas in high voltage circuit breakers and many other applications in high voltage technology is Sulphur Hexafluoride (SF_6) due to its unique insulating properties. However, it is a strong green house gas with a global warming potential of 23900 times that of CO_2 on a 100 year horizon [15]. Furthermore, it produces highly toxic components under switching operation.

The search for an alternative gas has revealed that CO_2 is a suitable replacement for SF_6 [14, 16–22]. ABB has introduced the first high voltage circuit breaker using CO_2 to the market [23]. The typical pressure range of CO_2 is then around 1 - 10 bar [14].

Knowledge on discharge dynamics in CO_2 is also

relevant for lightning on Venus that has an atmosphere of 96.5% CO_2 and 3.5% N_2 . While no optical signature of lightning activity has been reported (probably due to the low luminosity of CO_2 discharges in the visible range, or due to the opacity of the dense Venus atmosphere), electromagnetic remote sensing indicates lightning at a similar frequency as on earth [24].

Experimental investigations of streamer stability field, streamer radius and streamer velocities in CO_2 at ambient temperature in the pressure range of 0.5 – 5 bar for both positive and negative polarities are presented in [14]. On the other hand, simulations of positive streamers in CO_2 have only been performed in [25]; the authors used 2D Cartesian particle-in-cell Monte Carlo and 2D Cartesian fluid simulations to study streamer branching; however a 2D Cartesian computation gives only a qualitative picture. In contrast, here we study the propagation of streamers in CO_2 with axisymmetric fluid simulations, and we study how the streamer properties depend on the gas composition, electric field and background electron density.

A major bottleneck in the study of positive streamers in pure CO_2 is that there seems to be no effective photo-ionization in that gas, as we review and discuss in section 2.2.1 of this paper. This is true as well for CO_2 with admixtures of other gases, in particular, of O_2 or of air. Therefore streamer propagation in CO_2 seems only understandable with some other source of free electrons ahead of the streamer, e.g., due to radiation or to previous discharges. Therefore we insert different values of background electron densities and study their effect on the streamer propagation. Without such an electron source, streamer inception in CO_2 will be difficult and streamer propagation erratic with multiple branching attempts, as is discussed further in section 3.1.

1.3. Positive streamers in other gases

Positive streamers depend essentially on three functions that are specific for the particular gas composition: on the electron mobility $\mu(E)$, on the effective ionization coefficient $\alpha_{\text{eff}}(E)$, and on the distribution of photoionization or possibly some other source of free electrons ahead of the ionization front. The breakdown field is defined as the field where $\alpha_{\text{eff}}(E) = 0$. But beyond this single value that sets a scale for the electric field, the functional dependence of electron mobility μ and effective ionization coefficient α_{eff} on the electric field E or the electron energy determines streamer properties like velocity, radius and maximal electric field at the tip, and electric field and electron density in the streamer interior. To compare how streamer properties depend on these functions, in this paper, we study streamers in air, in CO_2 , and in CO_2 with

1% or 10% admixture of O₂ at standard temperature and pressure. (Note that other gas densities with the same mixture ratios can be approximated by scaling laws [3, 26]).

1.4. Contents of the paper

The structure of paper is as follows: Section 2 is devoted to the plasma fluid model with initial and boundary conditions. Subsection 2.2 reviews the literature on photoionization in air, in pure CO₂, and in CO₂ with admixtures of oxygen, air and other gases. Transport and reaction parameters for air and for CO₂ with or without admixture of oxygen are provided in section 2.3. In section 3, first the difficult propagation of CO₂ streamers without background ionization is discussed, and a first view on streamers in air and in CO₂ is given. Then the effect of replacing photoionization by background ionization in air streamers is discussed in section 3.3. In section 3.4, we characterize CO₂ streamers, and in section 3.5 streamers in air are compared to those in CO₂. The effect of oxygen admixture of 1% or 10% on CO₂ streamers are presented in section 3.6. Finally, the concluding remarks are presented in section 4.

2. Discharge model and conditions

We use a plasma fluid model for the densities of electrons and ions that incorporates elastic and inelastic collisions of electrons with O₂, N₂ and CO₂ molecules, including impact ionization and electron attachment reactions. Details on the calculation of mobility and reaction rates are given in section 2.3. Ions are considered immobile during the initial streamer phase due to their larger mass. For each gas we consider the respective reactions that are listed in table 1. Note that the rates of the three-body attachment reaction, $e + O_2 + M \rightarrow O_2^- + M$ with $M = N_2$, are about three orders of magnitude smaller than the respective rates for $M = O_2$ [27]. Therefore, we only consider the three-body attachment with $M = O_2$.

The model is implemented in Afivo-streamer [28]. It is based on the Afivo framework [29], which contains geometric multigrid techniques to solve the Poisson equation, octree-based adaptive mesh refinement (AMR) and OpenMP parallelism. The fluid equations are solved using explicit second order time stepping, and a slope-limited second order accurate spatial discretization.

2.1. Model equations

The electron density n_e evolves in time as

$$\partial_t n_e = \nabla \cdot (n_e \mu_e \mathbf{E} + D_e \nabla n_e) + S_i + S_{ph} - S_{attach}, \quad (1)$$

1	$e + CO_2 \rightarrow e + e + CO_2^+$	$k_1(E/N)$
2	$e + N_2 \rightarrow e + e + N_2^+$	$k_2(E/N)$
3	$e + O_2 \rightarrow e + e + O_2^+$	$k_3(E/N)$
4	$e + O_2 + O_2 \rightarrow O_2^- + O_2$	$k_4(N, E/N)$
5	$e + O_2 \rightarrow O^- + O$	$k_5(E/N)$
6	$e + CO_2 \rightarrow CO + O^-$	$k_6(E/N)$

Table 1: List of ionization and attachment reactions in the model used for the different gas compositions. The reaction rates depend on the reduced electric field E/N (where E is the field and N the gas density). They are calculated from elastic and inelastic cross sections as explained in section 2.3, and they are provided as input files to the fluid model. Reaction 4 also depends on the O₂ density, or on the gas density N , when assuming a constant fraction of O₂.

where μ_e is the (positive) electron mobility, D_e the electron diffusion coefficient, \mathbf{E} the electric field, S_i the impact ionization source term, S_{attach} the electron attachment source term, and S_{ph} the non-local photoionization source term (see section 2.2.1). All mobility and reaction coefficients are calculated in local field approximation.

The total positive ion density n_i^+ and the total negative ion density n_i^- change in time as

$$\partial_t n_i^+ = S_i + S_{ph}, \quad (2)$$

$$\partial_t n_i^- = S_{attach}. \quad (3)$$

The electric field is computed in electrostatic approximation as

$$\begin{aligned} \mathbf{E} &= -\nabla \phi, \\ \nabla^2 \phi &= -\frac{q}{\epsilon_0}, \quad q = e(n_i^+ - n_i^- - n_e), \end{aligned}$$

where ϕ is the electric potential, ϵ_0 the vacuum permittivity, q the space charge density and e the elementary charge. The impact ionization and the electron attachment source terms are computed according to

$$S_i = n_e[CO_2]k_1 + n_e[N_2]k_2 + n_e[O_2]k_3, \quad (4)$$

$$S_{attach} = n_e[O_2]^2 k_4 + n_e[O_2]k_5 + n_e[CO_2]k_6, \quad (5)$$

where [...] indicates the density of the respective species, and k_j , $j = 1, 2, \dots, 6$ are the respective reaction rates that still depend on the specific gas composition, as discussed further in section 2.3. For further reference, we recall that the ionization energies of O₂, N₂ and CO₂ are 12.1 eV, 15.6 eV and 13.8 eV [30].

2.2. Photoionization

2.2.1. Air For positive streamers in air, photoionization provides the free electrons in front of the streamer

head [5, 6] that are needed for streamer propagation into gases without preionization. It is generally accepted that photoionization in air occurs when excited nitrogen molecules emit radiation, which is absorbed by oxygen molecules and ionizes them. According to Zheleznyak *et al* [31] the wavelength of such radiation is in the 98 to 102.5 nm range; in this band the photon energy exceeds the ionization energy of 12.1 eV of O₂, and the photon absorption by nitrogen molecules is negligible.

When the photons are emitted isotropically and not scattered in the medium, and when the photon travel time is negligible, the photo-ionization source term $S_{\text{ph}}(\mathbf{r})$ can be written for each photon wave length as

$$S_{\text{ph}}(\mathbf{r}) = \int d^3\mathbf{r}' \frac{I(\mathbf{r}')f(|\mathbf{r} - \mathbf{r}'|)}{4\pi|\mathbf{r} - \mathbf{r}'|^2}. \quad (6)$$

Here $I(\mathbf{r})$ is the source of ionizing photons, $4\pi|\mathbf{r} - \mathbf{r}'|^2$ is a geometric factor, and $f(r)$ is the absorption function.

In Zheleznyak's model an effective function $f(r)$ for the wave length range of 98 to 102.5 nm is given by

$$f(r) = \frac{\exp(-\chi_{\min}p_{O_2}r) - \exp(-\chi_{\max}p_{O_2}r)}{r \ln(\chi_{\max}/\chi_{\min})}, \quad (7)$$

where $\chi_{\max} \approx 1.5 \times 10^2/(\text{mm bar})$, $\chi_{\min} \approx 2.6/(\text{mm bar})$, and p_{O_2} is the partial pressure of oxygen. Zheleznyak's UV photon source term $I(\mathbf{r})$ is proportional to the electron impact ionization source term S_i as given in equation (4)

$$I(\mathbf{r}) = \frac{p_q}{p + p_q} \xi S_i, \quad (8)$$

where the factor $p_q/(p + p_q)$ accounts for the collisional quenching of the excited nitrogen molecules, where p is the actual gas pressure and p_q a gas specific quenching pressure. In air at standard temperature and pressure, the corresponding absorption lengths are $[\chi_{\min}p_{O_2}]^{-1} = 1.9 \text{ mm}$ and $[\chi_{\max}p_{O_2}]^{-1} = 33 \text{ }\mu\text{m}$. The proportionality factor ξ , which relates the impact excitation to the impact ionization, is in principle field-dependent [31], but in this paper, we set it to $\xi = 0.05$. Furthermore, we use a quenching pressure of $p_q = 40 \text{ mbar}$.

Having the UV photon source term calculated, we evaluate the integral in equation (6) by using a set of Helmholtz differential equations [32, 33] with Bourdon's three-term parameters [32]. Besides to the original papers, the reader is referred to [34] and the appendix of [35] for more details.

2.2.2. CO₂ Even though there have been many studies on the physics of photoionization in air as well as on its numerical implementation in discharge models [30, 32, 33, 36, 37], to the best of our knowledge there are no quantitative photoionization models for discharges in CO₂ and CO₂ containing gas mixtures.

Direct measurements of absorption coefficients in CO₂ were only reported by Przybylski [38] and Teich [39] and retrieved by Pancheshnyi [30]; they are in the range of $0.34 - 2.2 \text{ cm}^{-1}\text{Torr}^{-1}$ ($= 25 - 165 \text{ mm}^{-1}\text{bar}^{-1}$), which at standard temperature and pressure correspond to absorption lengths in the range of $6.1 - 40 \text{ }\mu\text{m}$. Pancheshnyi [30] attributed these values to the spectral range of $83 - 89 \text{ nm}$, emitted by the dissociative ionization excitation products of CO₂ [40, 41]. The lower energy threshold to generate such products is about 50 eV [40], hence not in a relevant energy regime for electrons in typical streamer discharges. Therefore, we expect negligible photoionization in pure CO₂.

The authors of [25] also neglected photoionization of CO₂, but with a different argument than above; and they included a quasi neutral plasma with density of $10^9 / \text{m}^3$ in their simulation.

2.2.3. CO₂ with admixtures of oxygen or air In commercial circuit breakers based on CO₂, there are various contaminations with air and other impurities as well as admixtures of other gases. In particular, an admixture of O₂ is used in a breaker to suppress soot formation from the CO₂ discharge.

Photoionization of CO₂ containing gas mixtures was studied in [42] and [43] with the purpose of improving the output power of TEA (Transversely Excited Atmospheric) CO₂ lasers by photo-ionization of the gas admixtures. The measurements of Seguin *et al* [43] for several gas mixtures (e.g. CO₂ - N₂ - He) indicated that the photo-electron density is reduced by increasing the CO₂ fractions.

In CO₂ with an admixture of air, the radiation in 98 - 102.5 nm range that is emitted by nitrogen molecules and ionizes oxygen molecules, can be absorbed by CO₂. According to figure 24 in [30], the absorption coefficient for such radiation by CO₂ is in range of $0.8 - 2 \text{ cm}^{-1}\text{Torr}^{-1}$ ($= 60 - 150 \text{ mm}^{-1}\text{bar}^{-1}$), corresponding to an absorption length in the range of $6.1 - 17 \text{ }\mu\text{m}$ at standard temperature and pressure), hence the effect is quite local when considered on the scale of intrinsic streamer lengths. Furthermore, absorption of radiation in this energy range does not lead to ionization, as the CO₂ ionization threshold is about 89 nm (13.8 eV) [30].

In oxygen, radiation originating from the dissociative excitation of oxygen can ionize oxygen molecules and may be important for streamers in pure oxygen if the electron energy distribution shifts such that there is a substantial number of electrons with energy above 20 eV. However, similar to the above, CO₂ molecules absorb this radiation after some tens of micrometers without being ionized.

More in general, in CO₂ dominated mixtures at

STP, the photon absorption length is smaller than about $40 \mu\text{m}$, at least in the photon energy range from 7.6 to 16.9 eV and probably up to higher energies, based on the shape of the absorption curve [30].

We conclude that in CO_2 admixed with air, oxygen or other admixtures, photoionization is not a relevant mechanism for streamer propagation because of the short absorption length of relevant photons in CO_2 . In this paper, for the simulation of positive streamers in CO_2 , and CO_2 admixed with 1% and 10% oxygen, we incorporate a background density of electrons and positive ions. Such a density could be present for example due to previous discharges in a repetitively pulsed system [44].

2.3. Transport and reaction parameters

Electron-neutral scattering cross sections for CO_2 are taken from IST-Lisbon database [45] and for O_2 and N_2 from Phelps database [46], retrieved in May 2019. All transport and tabulated rate constants are calculated with BOLSIG+ [47], using the default temporal growth model.

The electron mobility μ_e , the diffusion coefficient D_e and the effective ionization coefficient $|\alpha_{\text{eff}}|$ at standard temperature and pressure are plotted in figure 1 for all gas mixtures considered in this paper. Here the effective ionization coefficient is defined as $\alpha_{\text{eff}} = \alpha - \eta$, where $\alpha = S_i / (n_e \mu_e |\mathbf{E}|)$ is the impact ionization coefficient and $\eta = S_{\text{attach}} / (n_e \mu_e |\mathbf{E}|)$ the attachment coefficient.

For CO_2 the electron mobility can be seen to be maximal at around 5.5 kV/cm [48]) and almost twice as high as in air. In the range of 5.5 kV/cm to 60 kV/cm, electrons in CO_2 have a higher diffusion coefficient than in air. Moreover, one can observe that the effective ionization coefficient in CO_2 is slightly higher than in air. The breakdown field, defined as the field where $\alpha = \eta$, is around 22 kV/cm for CO_2 and 28 kV/cm for air, both at STP. By including 10% or 1% of O_2 into CO_2 , the overall behavior of the parameters does not change, however the values are slightly changed. This shows that the reaction and transport coefficients in the studied gases are dominated by the majority molecule, CO_2 .

2.4. Computational domain and initial conditions

The computational domain shown and described in figure 2 is used for axisymmetric simulations. A potential difference of Φ_0 is applied over a distance of $z = 6.4 \text{ cm}$, creating a homogeneous background electric field. In this paper we employ different values for Φ_0 . This leads to different background electric fields, which are indicated explicitly in each section.

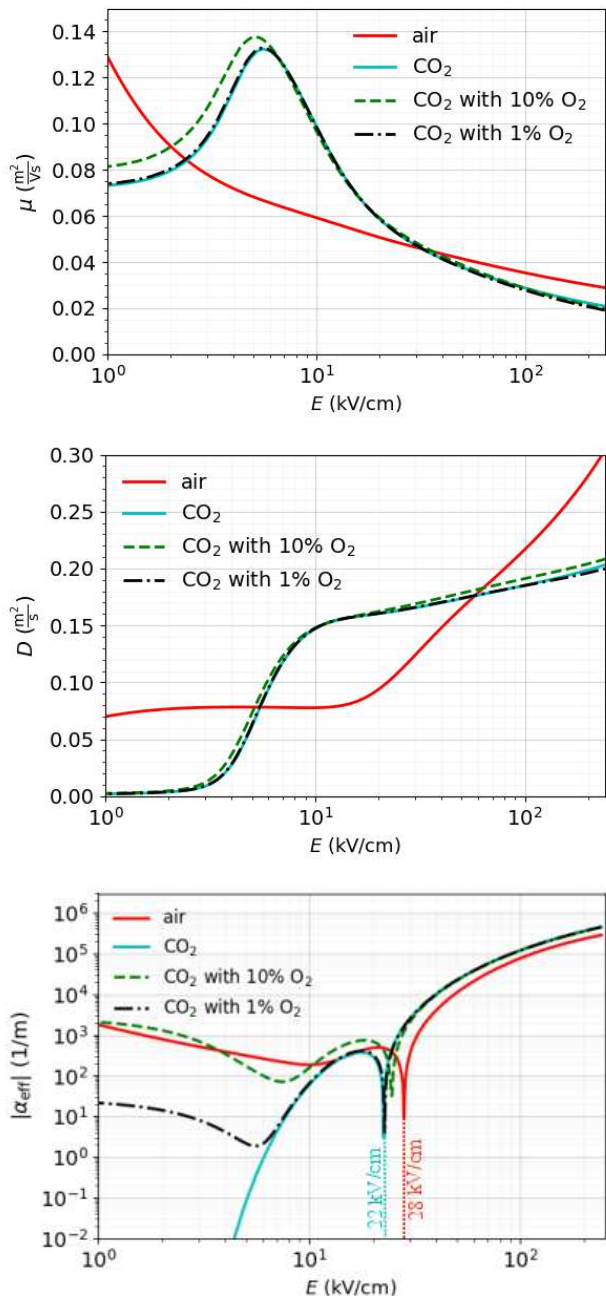


Figure 1: The electron mobility (top), the diffusion coefficient (middle), and the effective ionization coefficient (bottom) at STP condition for air, CO_2 , and CO_2 with 1% or 10% of O_2 . The breakdown field for air is $E_k^{\text{air}} = 28 \text{ kV/cm}$ and for CO_2 $E_k^{\text{CO}_2} = 22 \text{ kV/cm}$.

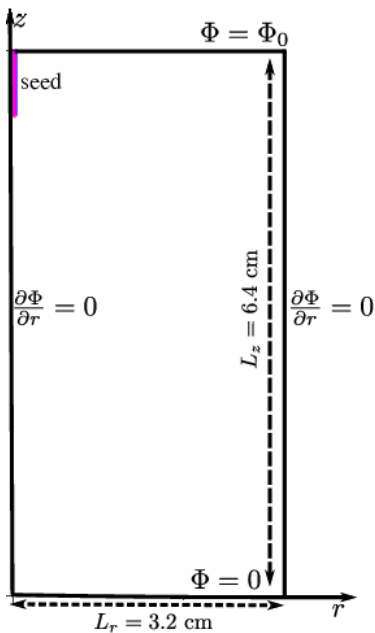


Figure 2: The axisymmetric domain extends over $0 \leq r \leq L_r = 3.2$ cm and $0 \leq z \leq L_z = 6.4$ cm. The position of the neutral seed on the axis of symmetry ($r = 0$) is indicated; the streamer starts from here. The boundary at $z = 6.4$ cm is on a potential $\Phi = \Phi_0$ and the boundary at $z = 0$ cm is grounded. For the potential, Neumann zero boundary conditions are used at $r = 0$ (imposed by symmetry), and at $r = L_r$. Neumann zero boundary conditions are also applied for the electron density on all boundaries.

We place a neutral seed of about 7.68 mm long with a radius of about 0.02 mm at the top boundary on the symmetry axis, $(r, z) = (0, 6.4)$ cm. The seed has an electron and positive ion density of $5 \cdot 10^{19} \text{ m}^{-3}$ at the center. This density decays with a smoothstep profile as $1 - 3l^2 + 2l^3$, where $l = \max[0, d/(0.1 \text{ mm}) - 1]$ and d is the distance to the line segment defining the seed.

In this paper, we use the same refinement criterion as in [28]. The grid is refined if $\alpha(1.2 \times E) \Delta x > 0.8$, where $\alpha(E)$ is the field-dependent ionization coefficient, E is the electric field strength, and Δx is the grid spacing. This gives an AMR grid with a minimum grid spacing of around $2 \mu\text{m}$.

3. Results and discussion

In section 3.1, we first discuss how the absence of effective photoionization in CO_2 can affect positive streamers, due to the lack of free electrons ahead of them. Afterwards, we compare streamer properties in air and CO_2 when a sufficient number of free electrons is available due to either background or

photoionization. A first overview of results is given in section 3.2. Several topics are then studied in more detail. In section 3.3, we compare the effect of photoionization versus background ionization in air. Next, the effect of different background ionization levels in pure CO_2 is studied in section 3.4, after which we compare the results in air and CO_2 in more detail. Finally, we present streamer simulations in CO_2 with an admixture of 1 or 10% of oxygen.

3.1. Positive streamers in CO_2 without background ionization

An important conclusion from section 2.2 is that there seems to be almost no photoionization in pure CO_2 or in CO_2 with a small admixture of oxygen or air. This could have a strong effect on positive streamers in such gases, since their growth depends on the presence of free electrons ahead of them. Such free electrons can also be provided by background ionization, e.g., by electron detachment from negative ions or by external radiation. However, without such electron sources, background ionization levels will be low [6]. In such cases, we expect several observable effects on positive streamers.

- The growth of the streamers would be highly irregular, as there would be few incoming electron avalanches, leading to a branched structure.
- Perhaps, the few incoming avalanches could become tiny negative streamers each extending the positive channel.
- The resulting discharge would have sharp features, leading to high local electric fields and an increased degree of ionization.

We are not aware of direct experimental evidence for such effects, probably because streamers in CO_2 emit little visible light. Some of the above effects have been observed in other gas mixtures with less photoionization than air [5, 49], such as N_2 with a small admixture of O_2 . Note that a distinguishing property of CO_2 is that it is both electronegative (unlike e.g. N_2 or Ar) and that it strongly absorbs the photons responsible for photoionization in air, ruling out photoionization due to air impurities.

Simulating positive streamers under the conditions outlined above is highly challenging, and outside the scope of the present paper. In the rest of the paper we therefore compare streamer properties in different gases with a sufficient number of free electrons available, and we test how sensitively our results depend on the assumed electron density.

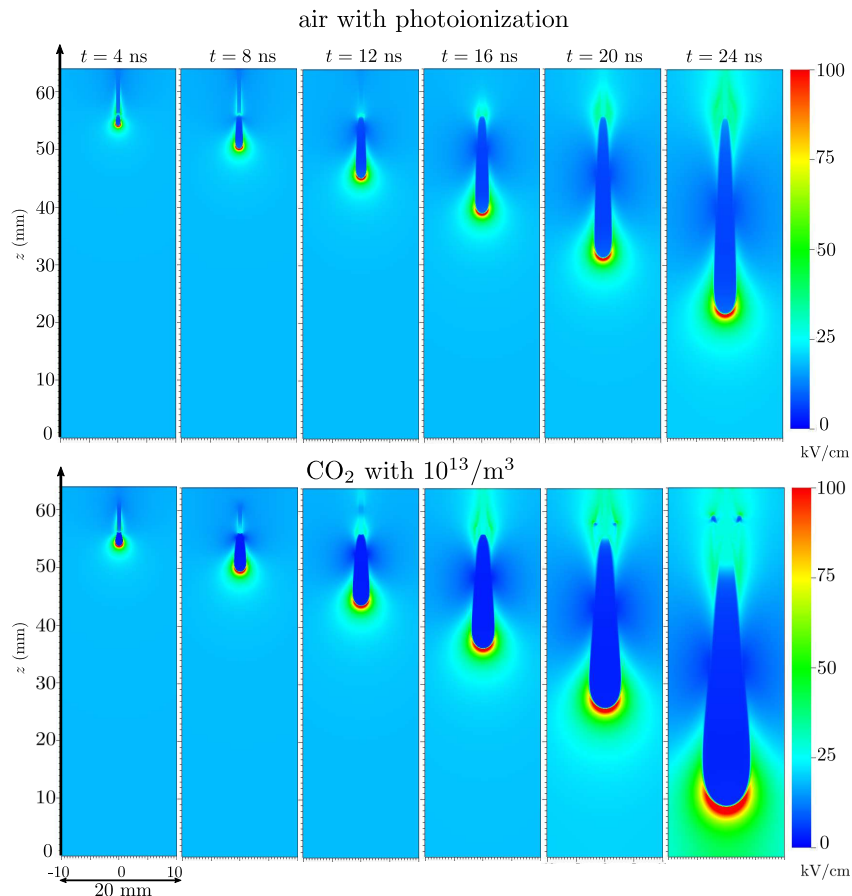


Figure 3: Time evolution of the electric field for the streamer in air (top) and in CO_2 (bottom) at standard temperature and pressure in a homogeneous electric field of 18 kV/cm. In the simulation of the air streamer, photoionization is included, whereas in the CO_2 streamer, a background electron density of $10^{13}/\text{m}^3$ is incorporated. The full gap length of 64 mm is shown. The simulation domain extends up to 32 mm in the radial direction, but only 10 mm are shown. The color-coding of the electric field strength is truncated for values above 100 kV/cm.

3.2. A first look at streamers in air and CO_2

In this section, we have a first look at streamer properties when a sufficient number of free electrons is available ahead of them. In CO_2 we provide such free electrons by adding a certain level of background ionization.

Figure 3 shows the dynamics of the streamer evolution in air (top) and in CO_2 (bottom) in a homogeneous electric field of 18 kV/cm. For the CO_2 streamer, a background density of free electrons and positive charges of $10^{13}/\text{m}^3$ is incorporated, whereas for the air streamer photoionization is included. Initially the electric field is enhanced at the location of the seed, and within a couple of nanoseconds a positive streamer propagates downwards. The air streamer bridges the gap after 30 ns and the CO_2 streamer after 25 ns. In this paper, we focus on the streamer propagation far from the electrodes, and we stop before

the streamer has reached the opposite electrode.

Figure 4 shows the electric field profile of the streamers in air and CO_2 when they have reached a fixed length. In the top row of panels a homogeneous electric field of 16 kV/cm is applied, in the middle row the field is 18 kV/cm and in the bottom row, it is 20 kV/cm. The results of air streamers with photoionization are included in the first column. In the other three columns, results in air and CO_2 with background ionization are shown, as indicated. To see the differences between the streamers more clearly, the electric field profiles are shown at the same streamer length, but at different times; these times are indicated in the top of each panel.

In what follows, we provide a detailed analysis of the properties of these streamers in air and in CO_2 .

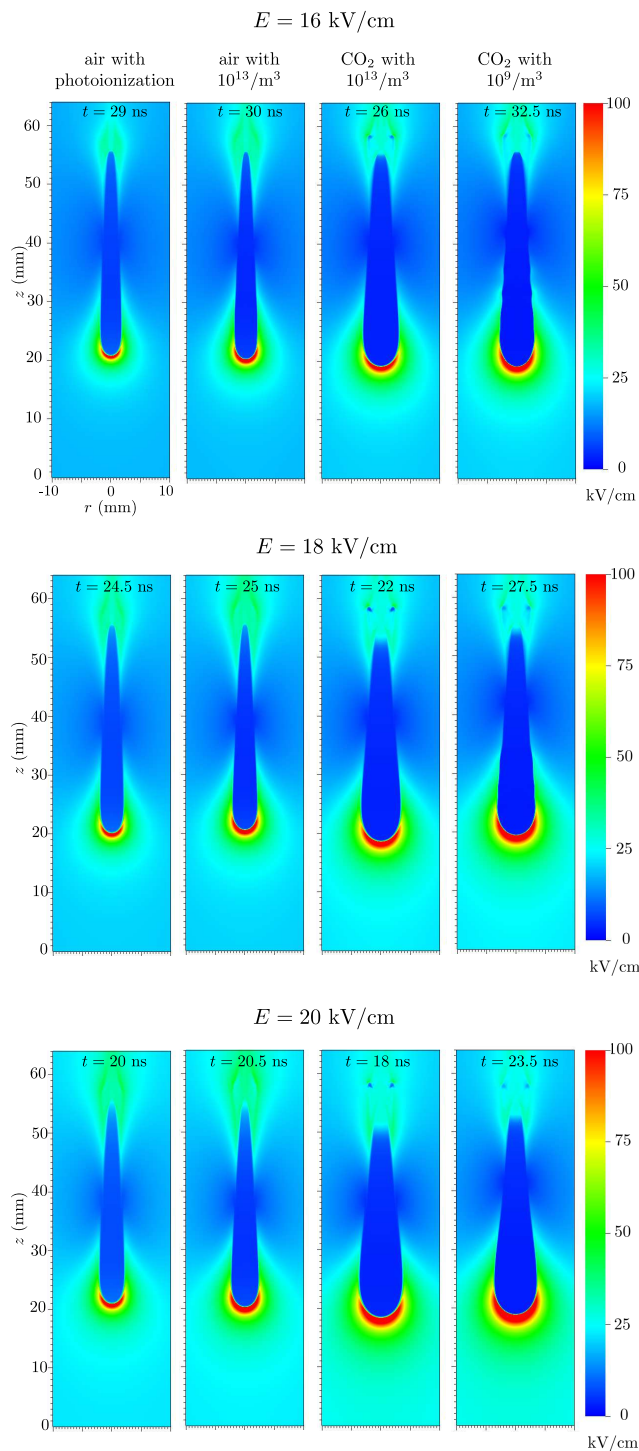


Figure 4: The electric field profile of the streamers in air and CO_2 when the streamer head is approximately at the coordinate $z = 20$ mm. The time when this coordinate is reached, is indicated at the top of each panel. The background electric field is $E = 16$ kV/cm (top), $E = 18$ kV/cm (middle), and $E = 20$ kV/cm (bottom). The inclusion of photoionization or background ionization is indicated above each column. The simulation domain extends up to 32 mm in the radial direction, but only 10 mm are shown.

3.3. Streamers in air: photoionization versus background ionization

In this section, we investigate the influence of photoionization versus background ionization and of the applied electric field on streamer properties in air. We performed two sets of simulations, where all the conditions are identical except that in one case we included photoionization in continuum approximation using Bourdon's three term parameters as described in section 2.2.1, and in the other case we incorporated a background ionization of $10^{13}/\text{m}^3$, but no photoionization.

The upper three panels in Figure 5 show the streamer velocity, maximal electric field, and radius versus streamer position for cases with photoionization or background ionization in three different applied electric fields. Here, the streamer position is defined as the z -coordinate where the electric field is maximal, and the streamer radius is defined as the radius where the radial component of the electric field is maximal. Note that these definitions are used throughout this paper. The initial transients during streamer formation for $z > 5$ cm are not shown in the figure, and the streamer propagates towards the lower electrode at $z = 0$. Boundary effects from approaching the electrode can be seen for $z \leq 1$ cm. The lower two panels in Figure 5 show on-axis electron density and electric field profiles along the z -axis when the streamer head is approximately at $z = 2$ cm. These two panels correspond to the left two columns of figure 4, where the times are indicated. The following observations can be made in the figure:

Velocity. As the streamers propagate, their velocities increase from 1×10^6 m/s to about 6×10^6 m/s. The streamer velocities coincide well until $z \approx 3$ cm. Then streamers with background ionization become faster in each external electric field, up to about 6% when approaching the opposite electrode. Moreover, the higher the electric field the faster the streamer travels.

Maximal electric field. During the initial streamer formation from the ionization seed, the maximal electric field briefly reaches about 200 kV/cm; this occurs for $z > 5$ cm and is not shown in the figure. Then, during the extended streamer propagation phase, the maximal electric field at the streamer head is about 145 – 160 kV/cm in cases with background ionization, and about 125 – 135 kV/cm in cases with photoionization. Hence, with background ionization the field is by about 20% larger. When the applied electric field is larger, the maximal field at the streamer head is larger as well for each streamer length. Oscillations are visible in the electric field (and other quantities) for the case with the lowest field and

background ionization; these oscillations are discussed below in section 3.3.1.

Radius. The streamer radius increases from about 0.5 mm to about 2.2 mm as it propagates between the two electrodes. It is about 10% larger in streamers with background ionization. Furthermore, for a larger applied electric field the radius is larger for each streamer length.

Electron density in the streamer interior. The streamers with background ionization have a larger electron density in the streamer interior than those with photoionization. They also have a higher maximal electric field at the streamer head. That a higher electric field at the tip creates a higher interior electron density, is established for negative streamers [50], but will require further investigations for positive streamers. There appear to be several competing effects here. Photoionization is strongest on-axis, which ‘focuses’ the growth of a positive streamer and therefore could explain the smaller radius with photoionization. Usually, a streamer with a smaller radius will have a stronger electric field at its tip. However, here the wider streamers with background ionization have stronger electric field enhancement. This is due to their higher electron density and thus also higher conductivity, for which we currently do not have a simple explanation.

Electric field in the streamer interior. The interior electric field on the axis is in the range of 4 – 5 kV/cm in simulations with background ionization and about 2 kV/cm larger in simulations with photoionization. Interestingly, the applied electric field has a very minor effect on the interior electric field. Apparently, the higher electron density in the interior supports larger screening currents that compensate for the higher fields at the tip. This is a topic of future investigations. The electric field of 5 kV/cm is sometimes attributed to the so called ‘*stability field*’ for positive streamers in air.

We conclude that the replacement of photoionization by a background electron density of $10^{13}/\text{m}^3$ in air provides a qualitative description of streamer properties. Both mechanisms create a sufficiently similar electron density profile in the active high field zone ahead of the streamer head within the parameter range explored in this paper.

3.3.1. Oscillations In figure 5 oscillations are visible in all quantities for the 16 kV/cm case with background ionization. Such oscillations were also observed in [35] when a background ionization level of $10^9/\text{m}^3$ was used to compare axisymmetric streamer codes. They

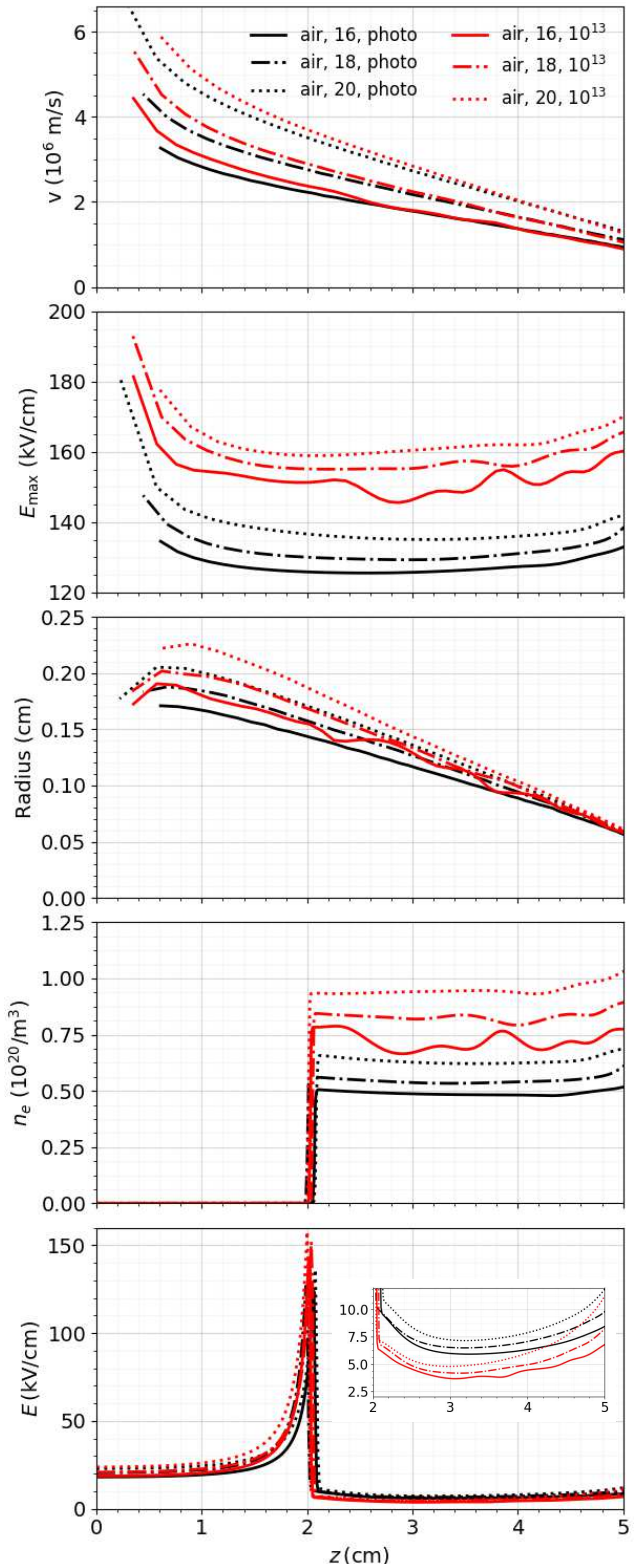


Figure 5: From top to bottom: streamer velocity, maximal electric field, and radius of the streamer head as a function of streamer position z ; and electron density and electric field on the z axis at the moment when the streamer head is approximately at $z = 2$ cm. The simulations are done here in dry air. The different lines indicate results with photoionization or with a background electron density of $10^{13}/\text{m}^3$ in applied electric fields of 16, 18 and 20 kV/cm.

were attributed to numerical effects as they could be removed by using a very fine grid and corresponding small time step. However, in our present simulations these oscillations did not disappear by reducing the grid size. After an extensive search, we did observe a sensitivity on the number of points in the tabulated input data. From this data, rate coefficients are determined by linear interpolation, which leads to small interpolation errors since processes like electron impact ionization are not linear in E/N . To reduce such interpolation errors, high-resolution input data with 200 entries was used for all simulations presented in this paper, but as shown in figure 5, some oscillations were nevertheless present.

The fact that small numerical or interpolation errors can cause oscillations in positive streamers indicates that these streamers are also ‘*physically*’ unstable to some degree. Our results show that this instability is enhanced when the applied field is reduced. A reduction in the background ionization level to $10^9/\text{m}^3$ (like in [35]) also led to significantly increased oscillations and branching. Since the axisymmetric fluid model used here is not suitable for the study of stochastic fluctuations or branching, we leave a further investigation of these effects to future work.

3.4. Streamers in CO_2 : different levels of background ionization

In this section, we characterize streamers in CO_2 . We studied the effect of different levels of background ionization on streamer properties to explore the sensitivity of the results to this parameter. In one set of simulations we included background ionization of $10^9/\text{m}^3$, and in another set background ionization of $10^{13}/\text{m}^3$. Streamers in CO_2 with background ionization of $10^9/\text{m}^3$ are more stable than in air; oscillations occur but the streamers do not branch.

In figure 6 the same functions are plotted as in figure 5, but now for streamers in CO_2 with a background ionization of $10^9/\text{m}^3$ or $10^{13}/\text{m}^3$. The same initial conditions are used and the same three electric fields are applied. The profiles of electron density and electric field on axis in the lower two panels of figure 6 show the same situation as the right two columns in figure 4. The following observations can be made:

Velocity. The streamer velocity increases in time from about $(1 - 1.5) \times 10^6$ m/s to $(4 - 4.5) \times 10^6$ m/s depending on the level of background ionization and on the applied electric field. By increasing the applied electric field from 16 to 20 kV/cm, the streamer velocity increases by up to 50 % for each streamer length. When the background electron density is

increased by 4 orders of magnitude, the streamer velocity for given streamer length varies by less than 10 %, i.e., it is very insensitive to such a large change.

Maximal electric field. During the streamer propagation phase, the maximal electric field at the streamer head is about 125 – 140 kV/cm in cases with background ionization of $10^{13}/\text{m}^3$ and it is about 150 – 165 in the cases with background ionization of $10^9/\text{m}^3$, i.e., it increases by about 25 % when the background electron density is reduced, but only by about 10 % when the applied electric field is increased.

Note that the maximal fields for streamers in applied fields of 16 and 18 kV/cm, and with background ionization of $10^9/\text{m}^3$ strongly oscillate. Such oscillations are discussed in section 3.3.1.

Radius. The streamer radius increases from about 0.8 mm to about 3.5 mm in time. It is somewhat higher for the higher background ionization and the higher applied electric fields.

Electron density in the streamer interior. As already said above, the electron density behind a negative streamer ionization front is determined by the maximal electric field at the streamer head [50]. A similar relation can be seen here for the positive streamers: the internal electron density depends more strongly on the shown levels of background electron density and more weakly on the applied electric field. This is the same functional dependence as for the maximal electric field discussed above.

Electric field in the streamer interior. The electric field on the axis is in the range of 2 – 3 kV/cm for $10^9/\text{m}^3$, and of 3 – 4 kV/cm for $10^{13}/\text{m}^3$. Again it only weakly depends on the applied electric field, but more strongly on the background electron density level.

Our main conclusion is that the streamer properties change only by up to 50 % and frequently much less, when the background electron density provided at the start of the simulation is changed from 10^9 to $10^{13}/\text{m}^3$, i.e., by 4 orders of magnitude. As a proper estimate of such a density is challenging, it is useful to note that the results on streamer propagation are rather insensitive to this parameter.

3.5. Air streamers versus CO_2 streamers

In this section, we compare streamers in air with those in CO_2 . A first view is already given in figure 4, where the CO_2 streamers are wider than air streamers for all values of the electric field. Furthermore, for the same background electron density and applied electric

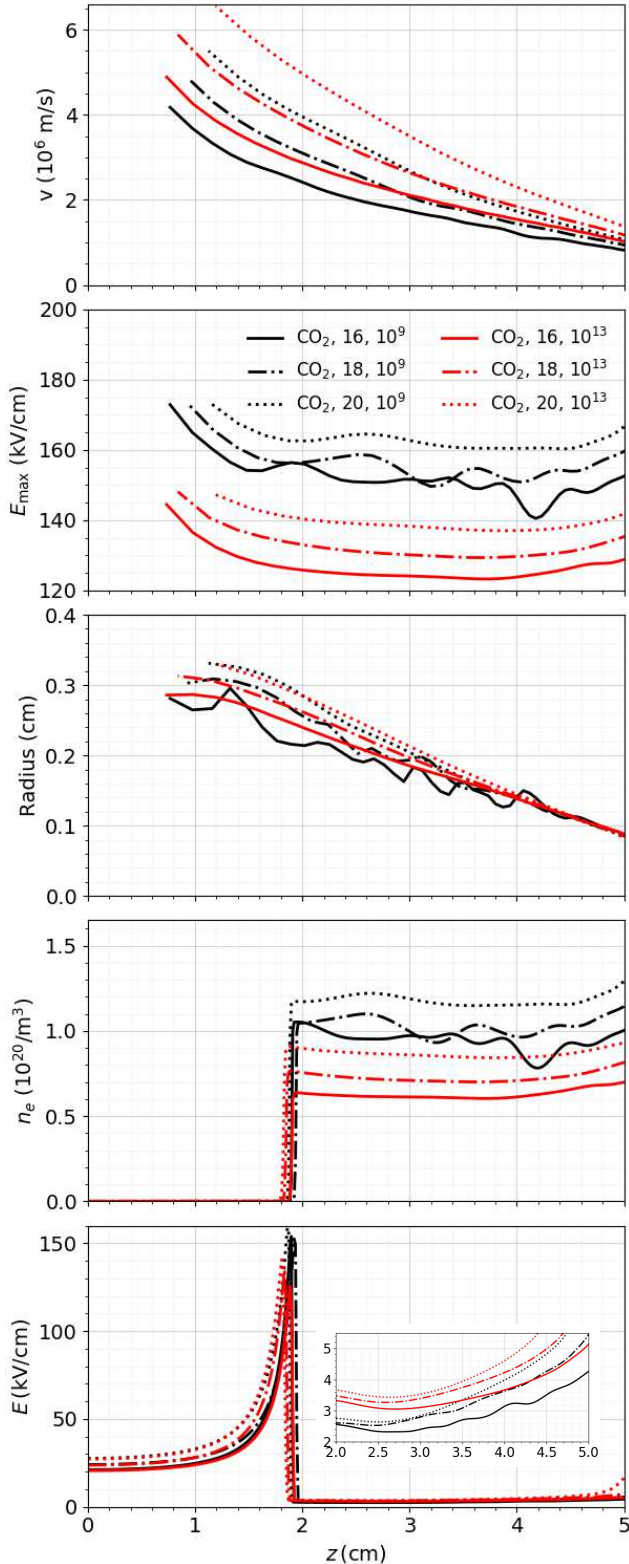


Figure 6: The same plots as in figure 5, now for CO₂. The different lines indicate results with background ionization of 10⁹/m³ and 10¹³/m³ in applied electric fields of 16, 18, and 20 kV/cm.

field, the CO₂ streamers are faster and they have a lower maximal electric field at their head. However, the fact that the CO₂ streamers are faster and wider could be due to the fact that the breakdown field E_k in air is 28 kV/cm and in CO₂ only 22 kV/cm. The fixed electric fields of 16 to 20 V/cm of the previous simulations are therefore closer to the breakdown field of CO₂.

Therefore, we here present simulations in air and in CO₂ at the same fraction $E = 0.73 E_k$ of their respective breakdown fields (hence for $E = 16$ kV/cm for CO₂ and $E = 20$ kV/cm for air), and with the same background electron density of 10¹³/m³. Figure 7 shows the same plots as the previous two figures for these two gases. According to Figure 4, the air streamer then has propagated for 20.5 ns, and the streamer in CO₂ for 26 ns.

Hence the air streamer now propagates about 30 % faster than the CO₂ streamer. The maximal electric field at the tip of the air streamer is about 35 kV/cm larger. And the streamer radius in air is about 15 % smaller. The interior electron density is larger in air than in CO₂. The interior electric field of air streamer reaches to a minimum value of about 5 kV/cm, whereas the interior electric field of the CO₂ streamer becomes as low as about 2.5 kV/cm.

3.6. Streamers in CO₂ with an oxygen admixture of 1% or 10%

As we mentioned in the introduction, in a circuit breaker, an admixture of O₂ is used to suppress soot formation in a CO₂ discharge. In this section, we investigate the effect of oxygen admixture of 10% and 1% on streamer properties in CO₂. We performed simulations using a background ionization of 10¹³/m³ and an applied electric field of 18 kV/cm. Figure 8 shows similar quantities as previous sections: the streamer velocity, maximal electric field, radius, and on-axis electron density and electric field profiles when the streamer is at about $z = 2$ cm. Streamer properties in CO₂ essentially do not change with an oxygen admixture of 1%. By increasing the oxygen admixture to 10% some small deviations start to appear. Most notable is the decay of the electron density on the streamer axis behind the ionization front in the case of the 10% O₂ admixture. This is due to the higher electron attachment rate (shown in Figure 1) in the streamer interior where the field is below 4 kV/cm.

4. Conclusion and outlook

We have presented simulations of the evolution of positive streamers in CO₂ and in air, with an emphasis on velocity, radius and maximal electric field at the streamer head, and on the generated electron

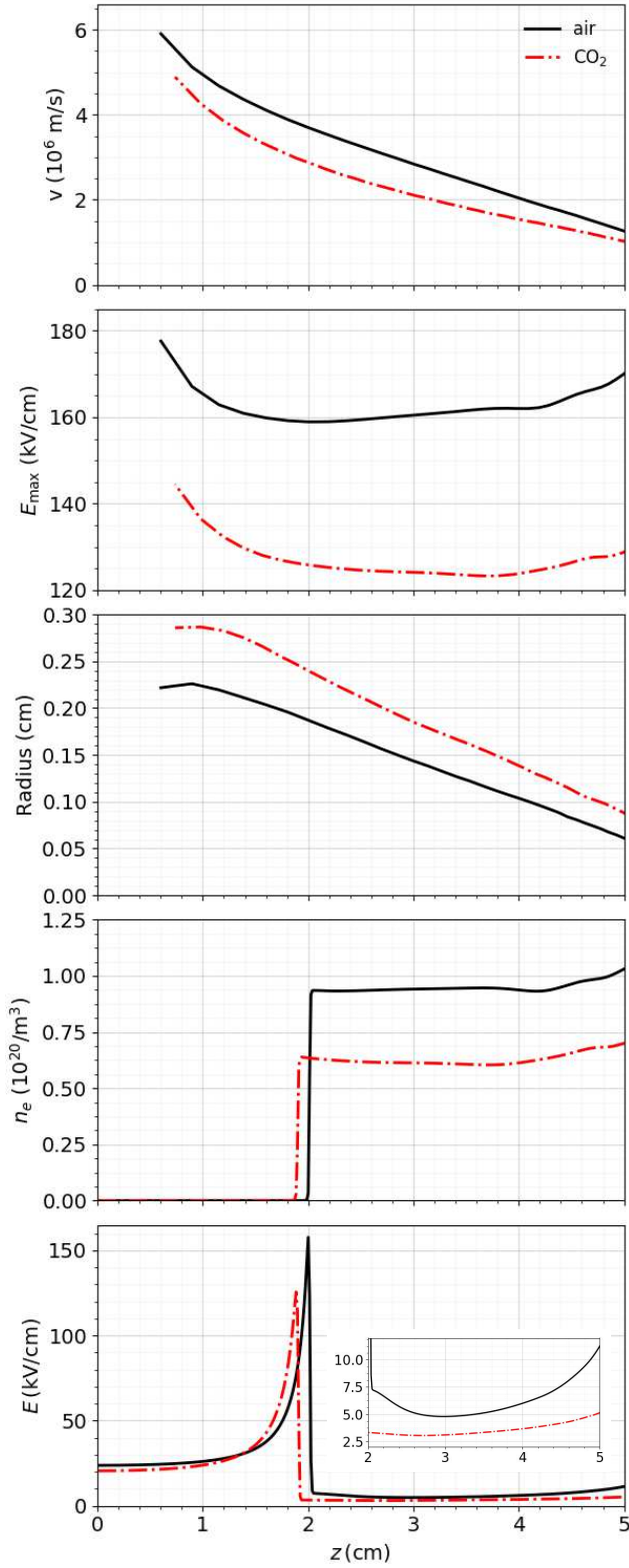


Figure 7: The same plots as in figure 5, now for air and CO_2 with background ionization of $10^{13}/\text{m}^3$ in an applied electric field of $E = 0.73 E_k$.

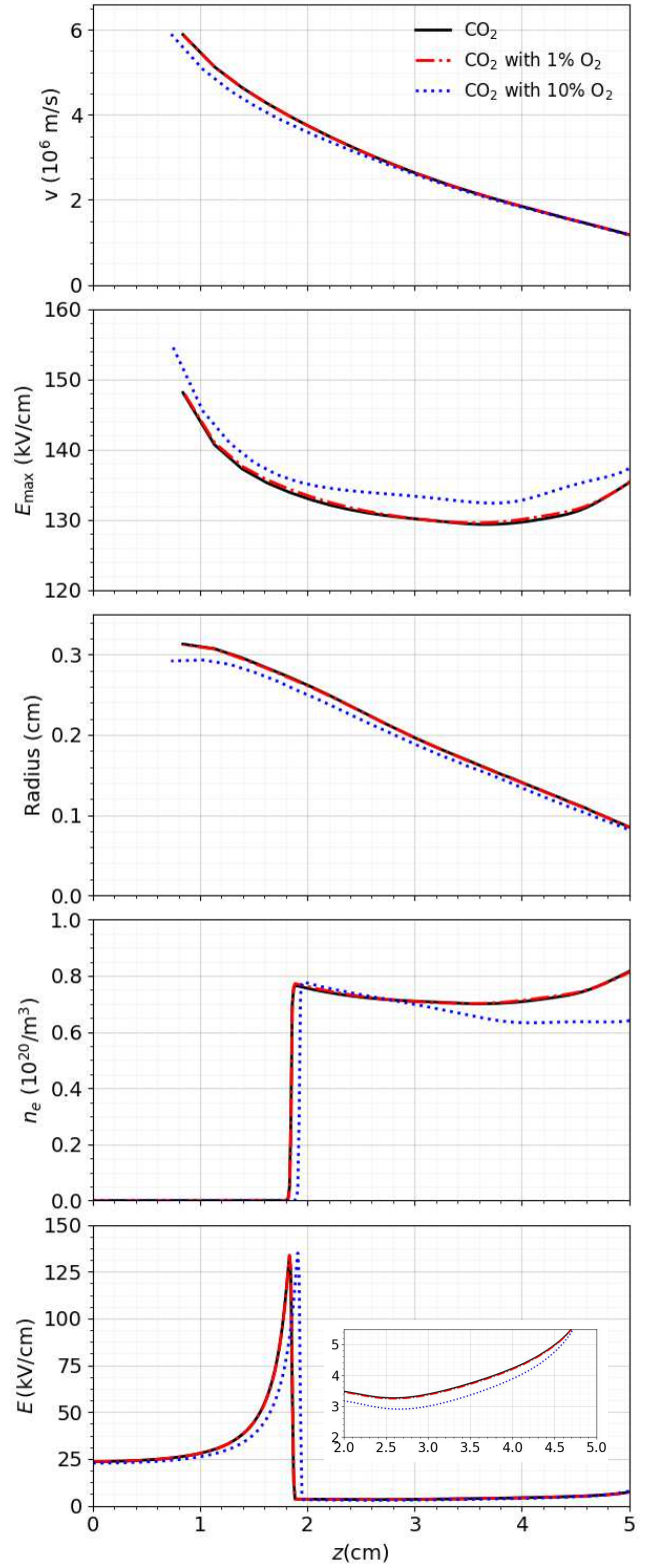


Figure 8: The same plots as in figure 5, now for pure CO_2 and for CO_2 with 1% or 10% of oxygen admixture. The applied electric field is $E=18 \text{ kV/cm}$, and background ionization is $10^{13}/\text{m}^3$.

density profile and the electric field inside the streamer channel.

4.1. Lack of photoionization in CO₂ containing gases

A major challenge for understanding positive streamers in CO₂ is that one needs a source of free electrons ahead of the ionization front for the streamer to propagate. In air, it is well established that photoionization provides such a source: for the typical electron energy distribution in a streamer ionization front, a wave length band of photons is generated that has sufficient energy to ionize an oxygen molecule, and that can propagate a distance of the order of a millimeter through air at standard temperature and pressure without being absorbed. Hence, photoionization in air provides a source of free electrons extending up to millimeters ahead of the ionization front. However, as we have reviewed in section 2, no such non-local electron source is known in CO₂. Rather, the CO₂ molecule absorbs photons in the relevant energy range after a few tens of micrometers. An admixture of oxygen or air does not help either as the photons relevant for the photoionization in nitrogen-oxygen mixtures are strongly absorbed by CO₂ as well.

A possible conclusion from this lack of non-local photoionization is that positive streamers in pure CO₂ or in CO₂ with admixtures of nitrogen and oxygen do not propagate at all, if there is no alternative source of free electrons ahead of the front. The consequences of such a lack of free electrons ahead of the streamer are described in section 3.1. As in air, such a source could be some background ionization due to previous discharges, or due to radioactive admixtures or other sources of external radiation.

4.2. Photoionization versus background ionization

Rather than searching for such specific sources, we have investigated the sensitivity of streamer simulations to photoionization or background ionization. Surprisingly, when photoionization in air is replaced by a background ionization of $10^{13}/\text{m}^3$ of free electrons and positive charges, the observed streamer parameters vary by no more than 20 % within the parameter range of our simulations.

Similarly, when we assume a density of 10^9 or $10^{13}/\text{m}^3$ of free electrons and positive charges in CO₂, the streamer properties (velocity, radius, maximal field, interior field and interior electron density) change by no more than 30%. From such a small change on a background electron density difference of 4 orders of magnitude, we conclude that the streamer properties during the propagation phase are rather insensitive to this parameter, hence we do not need to know it with high precision within the parameter range of our

simulations. However, we expect streamer inception and branching to depend strongly on this density.

4.3. The effect of transport and reaction parameters

The internal streamer dynamics is characterized not only by this free electron source, but also by the electron mobility μ and by the effective ionization coefficient α_{eff} . The breakdown field is the field where α_{eff} vanishes. However, when the background field is chosen as the same fraction of the breakdown field both in air and in CO₂ and when a background electron density of $10^{13}/\text{m}^3$ and no photoionization is used in both gases, the discharges are still not equal. Rather the air streamers have a larger velocity, a larger maximal electric field at the head, a larger interior electron density and electric field and a smaller radius. This is caused by the different functional dependence of μ and α_{eff} on the electric field, as shown in Fig. 1. An important difference is that the electron mobility is substantially larger in the interior of a CO₂ streamer, but somewhat lower in the active high field zone ahead of the streamer. Furthermore, the electron attachment rate in the interior of a CO₂ streamer is substantially lower than in air for fields below 10 kV/cm.

The non-linear evolution of streamer discharges makes it difficult to directly relate the observed differences to these transport coefficients. For example, a smaller radius and lower interior mobility reduce the conductivity of streamers in air, but the higher interior electron density in air has the opposite effect. The effect of the lower attachment rate in CO₂ is more clear: streamers in CO₂ will retain their conductivity for longer times/distances. This could partially explain why they obtain a larger radius in our simulations.

4.4. Quantitative results

- Replacing photoionization by a background electron density in simulations of air streamers does not drastically change streamer properties, at least within our sets of parameters.
- Streamers in air propagate faster than in CO₂ in a background electric field of 0.73 times the breakdown field of the respective gas. However, in a background electric field of 18 kV/cm streamers are faster in CO₂ than in air.
- The interior electric field in CO₂ streamers is about 2 – 4 kV/cm, whereas in air it is about 4 – 7 kV/cm. The applied electric field has a very minor effect on the interior field. At least in air streamers the inclusion of background ionization instead of photoionization reduces the interior electric field.
- The streamer properties in CO₂ are essentially unchanged when 1% or 10% of oxygen is admixed.

4.5. Outlook

We list here a number of questions left for future studies:

- Did we miss some possible source of free electrons ahead of a positive streamer in CO₂? Or can we find experimental observations where such a streamer really does not propagate?
- Can we estimate the free electron density in repetitive discharges in CO₂ for use in simulations?
- Can we derive some more quantitative understanding of the relation between the transport and reaction parameters $\mu(E)$ and $\alpha_{\text{eff}}(E)$ and the streamer properties?
- We tested background electric fields of 16 to 20 kV/cm where the streamers are expanding and accelerating. Will the same conclusions as above hold in lower electric fields or in longer gaps?

Acknowledgments

We acknowledge numerous fruitful discussion with Martin Seeger and his colleagues at ABB Corp. Res., Baden, Switzerland, as well as with our experimental collaborators at Eindhoven Univ. Techn. B.B. acknowledges funding through the Dutch STW-project 15052 “Let CO₂ spark!”.

Supplementary material

The simulation code used in this paper is available at <https://gitlab.com/MD-CWI-NL/afivo-streamer>. Moreover, the tabulated transport and rate constants, and the input files for generating the results together with the output files will be provided online, when the paper is accepted.

References

- [1] Vitello P A, Penetrante B M and Bardsley J N 1994 *Physical Review E* **49** 5574–5598 ISSN 1095-3787 URL <http://dx.doi.org/10.1103/PhysRevE.49.5574>
- [2] Yi W J and Williams P F 2002 *J. Phys. D: Appl. Phys.* **35** 205–218 ISSN 1361-6463 URL <http://dx.doi.org/10.1088/0022-3727/35/3/308>
- [3] Ebert U, Nijdam S, Li C, Luque A, Briels T and van Veldhuizen E 2010 *Journal of Geophysical Research* **115** ISSN 0148-0227 URL <http://dx.doi.org/10.1029/2009JA014867>
- [4] Nijdam S, Teunissen J and Ebert U 2020 *Plasma Sources Sci. Technol.*, in press URL <https://doi.org/10.1088/1361-6595/abaa05>
- [5] Nijdam S, van de Wetering F M J H, Blanc R, van Veldhuizen E M and Ebert U 2010 *J. Phys. D: Appl. Phys.* **43** 145204 ISSN 1361-6463 URL <http://dx.doi.org/10.1088/0022-3727/43/14/145204>
- [6] Pancheshnyi S 2005 *Plasma Sources Sci. Technol.* **14** 645–653 ISSN 1361-6595 URL <http://dx.doi.org/10.1088/0963-0252/14/4/002>
- [7] Fridman A, Chirokov A and Gutsol A 2005 *Journal of Physics D: Applied Physics* **38** R1–R24 ISSN 1361-6463 URL <http://dx.doi.org/10.1088/0022-3727/38/2/R01>
- [8] Adamovich I, Baalrud S D, Bogaerts A, Bruggeman P J, Cappelli M, Colombo V, Czarnetzki U, Ebert U, Eden J G, Favia P and et al 2017 *Journal of Physics D: Applied Physics* **50** 323001 ISSN 1361-6463 URL <http://dx.doi.org/10.1088/1361-6463/aa76f5>
- [9] Kanazawa S, Kawano H, Watanabe S, Furuki T, Akamine S, Ichiki R, Ohkubo T, Kocik M and Mizeraczyk J 2011 *Plasma Sources Science and Technology* **20** 034010 ISSN 1361-6595 URL <http://dx.doi.org/10.1088/0963-0252/20/3/034010>
- [10] Starikovskaia S M 2014 *J. Phys. D: Appl. Phys.* **47** 353001 ISSN 1361-6463 URL <http://dx.doi.org/10.1088/0022-3727/47/35/353001>
- [11] Nozaki T and Okazaki K 2013 *Catalysis Today* **211** 29–38 ISSN 0920-5861 URL <http://dx.doi.org/10.1016/j.cattod.2013.04.002>
- [12] Nakanishi K 1991
- [13] Ryan H M and Jones G R 1989 *SF6 switchgear* vol 10 (IET)
- [14] Seeger M, Avaheden J, Pancheshnyi S and Votteler T 2016 *Journal of Physics D: Applied Physics* **50** 015207 URL <https://doi.org/10.1088/2F1361-6463%2F50%2F1%2F015207>
- [15] 2014 United Nations Framework Convention on Climate Change <https://unfccc.int/process/transparency-and-reporting/greenhouse-gas-data/greenhouse-gas-data-unfccc/global-warming-potentials>,
- [16] Singhasathien A, Pruksanubal A, Tanthanuch N and Rungsevijitprapa W 2013 Dielectric strength of breakdown voltage of nitrogen and carbon-dioxide 2013 10th International Conference on Electrical Engineering/Electronics, Computer, Telecommunications and Information Technology (IEEE) pp 1–5
- [17] Okubo H and Beroual A 2011 *IEEE Electrical Insulation Magazine* **27** 34–42
- [18] Uchii T, Hoshina Y, Mori T, Kawano H, Nakamoto T and Mizoguchi H 2004 Investigations on sf 6-free gas circuit breaker adopting co 2 gas as an alternative arc-quenching and insulating medium *Gaseous Dielectrics X* (Springer) pp 205–210
- [19] Uchii T, Hoshina Y, Miyazaki K, Mori T, Kawano H, Nakamoto T and Hirano Y 2004 *IEEE Transactions on Power and Energy* **124** 476–484
- [20] Uchii T, Kawano H, Nakamoto T and Mizoguchi H 2004 *IEEE Transactions on Power and Energy* **124** 469–475
- [21] Seeger M 2015 *Plasma Chemistry and Plasma Processing* **35** 527–541
- [22] Stoller P C, Seeger M, Iordanidis A A and Naidis G V 2013 *IEEE Transactions on Plasma Science* **41** 2359–2369
- [23] <https://new.abb.com/high-voltage/AIS/selector/LTB-AirPlus>,
- [24] Dubrovin D, Nijdam S, Van Veldhuizen E, Ebert U, Yair Y and Price C 2010 *Journal of Geophysical Research: Space Physics* **115**
- [25] Levko D, Pachuilo M and Raja L L 2017 *Journal of Physics D: Applied Physics* **50** 354004 ISSN 1361-6463 URL <http://dx.doi.org/10.1088/1361-6463/aa7e6c>
- [26] Briels T M P, van Veldhuizen E M and Ebert U 2008 *J. Phys. D: Appl. Phys.* **41** 234008 ISSN 1361-6463 URL <https://doi.org/10.1088/0022-3727/41/23/234008>
- [27] Kossyi I A, Kostinsky A Y, Matveyev A A and Silakov V P 1992 *Plasma Sources Sci. Technol.* **1** 207–220 ISSN 1361-6595 URL <http://dx.doi.org/10.1088/0963-0252/1/>

3/011

- [28] Teunissen J and Ebert U 2017 Journal of Physics D: Applied Physics **50** 474001 ISSN 1361-6463 URL <http://dx.doi.org/10.1088/1361-6463/aa8faf>
- [29] Teunissen J and Ebert U 2018 Computer Physics Communications **233** 156–166 ISSN 0010-4655 URL <http://dx.doi.org/10.1016/j.cpc.2018.06.018>
- [30] Pancheshnyi S 2015 Plasma Sources Sci. Technol. **24** 015023 ISSN 1361-6595 URL <http://dx.doi.org/10.1088/0963-0252/24/1/015023>
- [31] Zheleznyak M B, Mnatsakanian A K and Sizykh S V 1982 Teplofizika Vysokikh Temperatur **20** 423–428
- [32] Bourdon A, Pasko V P, Liu N Y, Célestin S, Ségur P and Marode E 2007 Plasma Sources Sci. Technol. **16** 656–678 ISSN 1361-6595 URL <http://dx.doi.org/10.1088/0963-0252/16/3/026>
- [33] Luque A, Ebert U, Montijn C and Hundsdoerfer W 2007 Appl. Phys. Lett. **90** 081501 ISSN 0003-6951 URL <http://dx.doi.org/10.1063/1.2435934>
- [34] Bagheri B and Teunissen J 2019 Plasma Sources Science and Technology **28** 045013
- [35] Bagheri B, Teunissen J, Ebert U, Becker M M, Chen S, Ducasse O, Eichwald O, Loffhagen D, Luque A, Mihailova D, Plewa J M, van Dijk J and Yousfi M 2018 Plasma Sources Science and Technology **27** 095002
- [36] Stephens J, Fierro A, Beeson S, Laity G, Trienekens D, Joshi R P, Dickens J and Neuber A 2016 Plasma Sources Science and Technology **25** 025024 ISSN 1361-6595 URL <http://dx.doi.org/10.1088/0963-0252/25/2/025024>
- [37] Stephens J, Abide M, Fierro A and Neuber A 2018 Plasma Sources Science and Technology **27** 075007 ISSN 1361-6595 URL <http://dx.doi.org/10.1088/1361-6595/aacc91>
- [38] Przybylski A 1967 Zeitschrift für Physik **25** 504–511
- [39] Teich T H 1967 Zeitschrift für Physik **199** 378–394 ISSN 1434-601X URL <http://dx.doi.org/10.1007/BF01332287>
- [40] Sroka W 1970 Zeitschrift für Naturforschung A **25** ISSN 1865-7109, 0932-0784 URL <https://www.degruyter.com/view/j/zna.1970.25.issue-10/zna-1970-1013/zna-1970-1013.xml>
- [41] van der Burgt P J M, Westerveld W B and Risley J S 1989 Journal of Physical and Chemical Reference Data **18** 1757–1805 ISSN 0047-2689, 1529-7845 URL <http://aip.scitation.org/doi/10.1063/1.555844>
- [42] Scott S J and Smith A L S 1982 Applied Physics Letters **41** 783–785 ISSN 0003-6951, 1077-3118 URL <http://aip.scitation.org/doi/10.1063/1.93702>
- [43] Seguin H, Tulip J and McKen D 1974 IEEE Journal of Quantum Electronics **10** 311–319 ISSN 0018-9197
- [44] Nijdam S, Takahashi E, Markosyan A and Ebert U 2014 Plasma Sources Sci. T. **23** 025008
- [45] Grofulović M, Alves L L and Guerra V 2016 Journal of Physics D: Applied Physics **49** 395207
- [46] Phelps database, retrieved May 2019 URL www.lxcat.net
- [47] Hagelaar G J M and Pitchford L C 2005 Plasma Sources Science and Technology **14** 722–733 ISSN 1361-6595 URL <http://dx.doi.org/10.1088/0963-0252/14/4/011>
- [48] Haefliger P and Franck C M 2018 Review of Scientific Instruments **89** 023114 (*Preprint* <https://doi.org/10.1063/1.5002762>) URL <https://doi.org/10.1063/1.5002762>
- [49] Teunissen J and Ebert U 2016 Plasma Sources Science and Technology **25** 044005 ISSN 1361-6595 URL <http://dx.doi.org/10.1088/0963-0252/25/4/044005>
- [50] Li C, Brok W J M, Ebert U and van der Mullen J J A M 2007 Journal of Applied Physics **101** 123305 ISSN 0021-8979 URL <http://dx.doi.org/10.1063/1.2748673>

This figure "diffusion.png" is available in "png" format from:

<http://arxiv.org/ps/2010.00926v1>